ISSN: 1813-4890

Structural Design and Discrete Element Process Simulation of Large Wet Horizontal Superfine Stirring Mill

Zhuangzhi Niu [1, a], Deyu Zhang [2, b]

[1]School of Mechanical and Power Engineering, Henan, Polytechnic University, Jiaozuo 454000, China;

[2]School of Mechanical and Power Engineering, Henan, Polytechnic University, Jiaozuo 454000, China.

[a]2543286960@qq.com

Abstract

With the realization of industrialization of submicron and ultramicron powder technology, the demand for high-efficiency and energy-saving large-scale wet horizontal ultrafine stirred mills has become urgent in fields such as metal industry and energy industry. This demand has given rise to some problems that have never been encountered or cannot be solved in large-scale machines and experimental research. This chapter uses the research results of predecessors to carry out the structural design of a large-scale wet horizontal ultrafine stirred mill, and conducts experimental research on the actual working conditions of the mill. At the same time, a discrete element simulation model of a large-scale wet horizontal ultrafine stirred mill is established to simulate the force and motion distribution of the grinding media in the mill under different operating conditions, and the crushing effect of materials in different areas of the mill is analyzed in combination with the analysis conclusions of single particle impact crushing .

Keywords

Stirring Mill, Discrete Element, Pellet Plant Distribution.

1. Introduction

After the physical analysis of the milled product, a mathematical quantitative analysis is essential to fully understand the operating state of each component in the mill. In this regard, the discrete element model (DEM) of the mill plays an important role and is used to answer some of the questions raised by the research objectives. DEM helps to evaluate the impact of material flow on the grinding effect under different operating conditions of the mill, as well as the distribution of different types of forces in the mill chamber.

There are many different approaches to choose from when building models such as mathematical models or computer simulations. Radziszewski and Morrell [1] developed a discrete element mathematical model of a ball mill. Datta and Rajamani [2] also modeled a ball mill, but used two-dimensional discrete element modeling (DEM). Govender and Powell [3] verified the correctness of the discrete element model based on the power obtained from three-dimensional particle tracking experiments. Zhao et al. [4] used discrete element modeling to model irregular shaped particles in three dimensions. Gui and Fan [5] studied the movement of rigid spherical particles in a rotating roller mill. Gers et al. [6] numerically simulated a stirred media mill and studied the grinding operation, fluid dynamics and collision characteristics of the mill. Mannheim [7] recently used an empirical mathematical modeling procedure to scale up a stirred ball mill. Cleary and Sinnott et al. [8] used DEM to model tower, pin and vertical stirred mills. They studied the media flow in the mill and the influence of hybrid meshes and force networks on the modeling accuracy during the modeling process. Positron emission particle tomography (PEPT) can be used to visualize the movement of particles in a mill. Conway et al. and Barley et al. [9] used PEPT as a tool for discrete element modeling of vertical stirred mills. Jayasundara et al. [10] used PEPT in the same way for discrete element modeling of horizontal stirred mills.

2. Research and development of large-scale wet-process horizontal ultrafine stirring mill

2.1. Basic requirements and intended use

The development of large-scale wet horizontal ultrafine stirred mill is mainly aimed at the wet grinding of titanium dioxide (titanium dioxide particles), and the specific requirements for it are as follows:

(1) Ensure that the particles in the mill cylinder flow evenly and smoothly, and the energy distribution in the grinding area is even;

(2) Large monomer volume processing capacity;

(3) Reduce energy consumption as much as possible;

(4) The equipment operates smoothly, safely and reliably.

2.2. Mill barrel design

After a lot of theoretical and experimental research, the ratio of the outer diameter of the dispersion disc to the inner diameter of the mill is determined to be 7:1~8.5:1, so as to ensure that the gap between the dispersion disc and the cylinder can ensure that the dispersion disc can drive the medium balls and materials to move, thereby improving the crushing effect, and will not cause excessive power consumption and affect the grinding effect. The cross-sectional area of the cylinder is circular, and the lining plate is lined with ceramic to increase wear resistance. In the design of the cylinder, the feed port, discharge port and discharge port are reasonably set. At the same time, considering the heating of the mill, the cylinder structure adopts a jacket form, and practice has proved that the cooling effect is good.

2.3. Agitator design

In the design process of large-scale wet horizontal ultrafine stirred mill , the design of the agitator is crucial. The agitator is a key component of the equipment. This mill adopts a disc stirring basic structure. The dispersion disc and the main shaft are made of special alloy wear-resistant materials to reduce wear and extend life. Through a large number of experimental studies and numerical simulation results, the structural parameters of the agitator are correctly determined. The determination principle is that the gap between the outer diameter of the agitator and the inner wall of the cylinder should be sufficient to prevent the ball from getting stuck, and make full use of the energy to transmit to the medium ball for movement. The size of the gap is affected by factors such as rotation speed, grinding media and agitator structure. The selection of the number of dispersion discs takes into account factors such as energy transmission frequency, medium filling amount, power transmission, grinding retention time , etc., and also takes into account the force of the agitator and the stability of the equipment.

3. Structure and experimental study of large-scale wet horizontal ultrafine stirred mill

The test run parameters of the mill are shown in Table 1. The running current of the mill is very stable, and the discharge temperature is kept within a very small range, which indicates that

ISSN: 1813-4890

the mill runs very smoothly. Although the running-in liquid level and flow rate fluctuate slightly, the effect on the grinding effect of titanium dioxide particles is minimal.

Table 1 Mill test run parameters

time	Grinding cylinder pressure (bar)	Host current (A)	Discharge temperature (℃)	Running-in level (mm)	flow m^3/h
7:30	0.2	164	44	3400	4.19
8:30	0.2	160	45	3700	3.91
9:30	0.2	166	45	4000	3.92
11:30	0.2	166	45	4300	4.1
12:30	0.2	165	45	4700	3.97

It can be seen from Table 2 that the feed particle size of titanium dioxide is about 0.5 mm, while the discharge fineness is maintained at 0.44 μm, which confirms that the independently designed mill has the same grinding effect as the mill produced on the market.

Table 2 Mill discharge fineness

Feed flow$\boldsymbol{m^3/h}$	Feed temperature ℃	Feed size $\boldsymbol{mm}$	Discharge temperature ℃	Discharge fineness$\boldsymbol{\mu m}$	Sealing liquid flow$\boldsymbol{L/min}$	Bead quantity t
4	40	0.581	44.5	0.475	3	1.39
4	39.9	0.532	46	0.448	3	1.39
4	40	0.431	46	0.442	3	1.5
4	39.9	0.436	50	0.447	3	1.5

According to Table 3, the temperature rise of each component inside the mill is within the controllable range of the design, which once again demonstrates the stability of the mill operation and the rationality of the design.

Table 3 Temperature data of each node of the mill

Bearings	Machinery Seal	Motor	Discharge pipe	Feed pipe
30.07	31.9	43.2	40.5	36.6
33.7	33.9	58	38.6	37.9
34.8	34.1	61	39.2	36.8
35.8	34.3	62	38.3	37

Fig. 1 shows the scanning electron microscope images of titanium dioxide particles before and after grinding. Figure 1 (a) and (b) are electron microscope images magnified 5000 times, from which it can be seen that the shape of the feed particles is regular, and the large and small particles are agglomerated together. Fig 1 (c) and (d) are electron microscope images magnified 20,000 times, and the diameter of the particles is significantly reduced, but there are still a small number of particles agglomerated together.

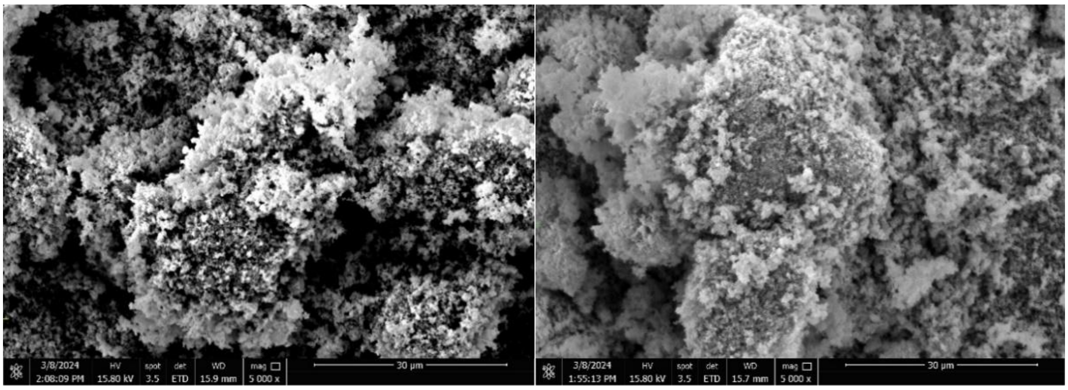

(a) Before grinding

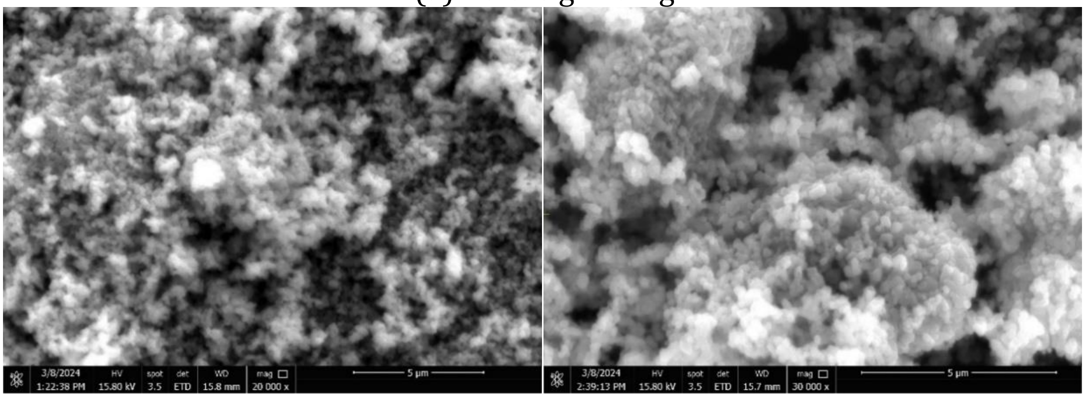

(b) After grinding

Fig 1 SEM images of titanium dioxide particles before and after grinding

Fig 2 Example of a large wet-process horizontal ultrafine stirring mill produced by a company

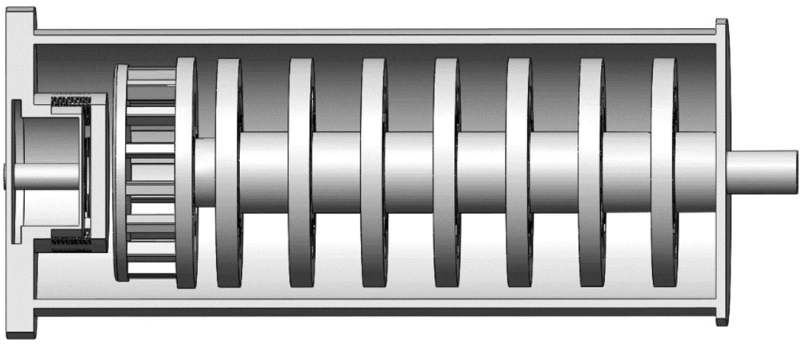

Fig 3 Geometric modeling of wet horizontal ultrafine stirred mill

4. Establishment of simulation model of large-scale wet horizontal ultrafine stirred mill

4.1. Establishment of mill geometry model

The model generates particles within the boundaries of the system, and the system can contain both stationary and moving parts. The geometric design of the system is similar to the structure of the actual machine, and the moving parts are assigned the magnitude and direction of the kinematic dynamics, which can be rotation, translation, or a combination thereof. If the geometric structure of the system consists of simple cylinders, cubes, and cuboids, the system can be created in the EDEM software. However, if the parts are more complex, they need to be imported from computer-aided design software (CAD) and the geometry is first drafted in the CAD software. In this study, the geometry and dimensions of the grinder are based on the actual production model provided by a company as shown in Fig 2. The geometric model of the agitator shaft and disc is shown in Fig 3, and the specific dimensions are shown in Table 4.

Table 4 Structural parameters of wet horizontal ultrafine stirring mill

parameter	symbol	Numeric
Dispersion disc diameter	D_s	790mm
Dispersion plate spacing	P	175 mm
Effective length of stirring shaft	H_s	2072.2 mm
Inner diameter of cylinder	D_b	930 mm
Cylinder length	H_b	2400 mm

The geometry of the mill agitator was drawn using SolidWorks CAD software and then imported into EDEM as the agitator geometry part of the mill.

The particle factory is a virtual geometry that surrounds the six disks of the agitator . Its function is to generate particles at random locations around the agitator and three disks in the grinding chamber. The geometry of the factory was pre-drawn using the same CAD software (SolidWorks). During the particle generation process, the factory has no physical influence on the interaction between particles. When particles are generated, the only force acting on the particles is caused by gravity. At the same time, a certain initial velocity is given to the particles, and the agitator is kept stationary for 0.5 seconds during the simulation time, so that the particles can settle under the influence of the initial velocity and gravity.

4.2. Establishment of the particle number model for mill discrete element simulation

The manufacturer recommends loading the grinding media to 80% of the effective volume of the mill. The effective volume is the volume of the grinding chamber, including the agitator and the dispersion disc, but excluding the last disc and the finger area (classifier area). To calculate the effective volume, the dimensions of the grinding chamber are used minus the agitator volume. Then, 80% of the net volume is used to fill the grinding media. The diameters of the actual grinding media particles and titanium dioxide particles are 1.5 mm and 0.5 mm, respectively. If the actual size of the grinding media particles were to be simulated, it would result in a large number of particles, in the order of tens of millions. In order to minimize the number of simulated particles and reduce simulation time, the smaller diameter titanium dioxide particles will be ignored and the diameter of the grinding media particles will be fixed to 10 mm.

According to the above standards, the grinding states when the particle filling amount is 50%, 60%, 80% and 90% are simulated, and the total number of corresponding particles is 68750, 82500, 110000 and 123750 respectively.

4.3. Establishment of material parameters for mill discrete element simulation

The different parts of the mill, including the agitator, chamber, and most importantly, the particles, have unique mechanical properties predefined by the user. The mechanical properties of the mill parts and particles directly affect the behavior and the resultant forces of the particles. The goal is to create a model that is as close to the real situation as possible. The materials of the mill barrel and grinding media are structural steel and zirconium dioxide, respectively, and the specific parameters are shown in Table 5.

Table 5 Discrete element simulation parameters of each component

	density (Kg/m^3)	Poisson's ratio	Shear modulus Pa	Elastic recovery coefficient	Static friction coefficient	Rolling friction coefficient
Structural Steel	7850	0.3	7.692×10^{10}	0.5	0.56	0.01
zirconium dioxide	3900	0.29	8.915×10^{10}	0.5	0.54	0.01

The iteration rate of the model was a major concern, as simulating a one-second run should not require a significant number of iteration times. The iteration rate is defined as the number of iteration hours per second of simulation. To address this, the media particles were assigned baseline material properties for the first simulation run, but this resulted in a very slow run rate, with an iteration rate of only 1 second of simulation per 27.6 hours of simulation. A series of simulation runs were performed to analyze the effect of the material properties on the particle behavior and the simulation iteration time.

4.4. Establishment of grinding mill discrete element simulation model parameters

Since the purpose of the model is to understand the behavior of particles in the mill under different operating conditions and how different particle characteristics affect each other, it is reasonable to divide the parameters into fixed and variable parameters.

The fixed parameters include mill structure design, material properties, contact force model, particle number and external forces acting on the particles. In order to achieve a realistic simulation based on reasonable values of the iteration parameters, these fixed parameters must be properly compromised.

The fixed parameters are summarized as follows:

(1) The grinding mill agitator disc is round.

(2) Input material properties into EDEM software.

(3) The interactions between particles and mill components are the coefficient of restitution, the coefficient of static friction and the coefficient of rolling friction.

(4) The particle size of the grinding medium is 10 mm, and the presence of titanium dioxide particles is ignored.

(5) The contact force model is the Hertz contact model.

The main objectives of the simulation are to visualize the behavior of the particles throughout the length of the mill and to quantify the forces experienced by the particles at different agitator speeds at different loading levels. The effect of agitator speed on a single material type in the mill (i.e., zirconia media particles) was tested by performing a series of simulation runs at three agitator speeds of 1000, 1500, and 2000 rpm. The effect was quantified by varying the agitator speed and analyzing its response. The rate at which the particles spread over the mill can be quantified and the type (normal/tangential) and magnitude of the forces generated at different input energies can be analyzed.

4.5. DEM simulation results of large-scale wet horizontal ultrafine stirred mill

4.5.1. Determination of simulation time step

In order to minimize the simulation time while ensuring the correctness of the simulation model, two simulation schemes with different time steps were used, as shown in Table 6. The data of the average grinding medium velocity, the average total energy, and the average compression force under the two schemes were compared, and it was found that when the time stepwas reduced from 1.78×10^{-5} s to 7.11209×10^{-7}s, the numerical difference between the three data was very small. However, the simulation time was reduced from 43 hours to 6 hours, so 1.78×10^{-5}s was selected as the standard time step of the simulation model.

Table 6 Comparison of simulation data at different time steps

Simulation time step (s)	Average speed (m/s)	Total energy mean (J)	Mean compression force (N)
7.11209×10^{-7}	5.3	1.47	36.3
1.78×10^{-5}	5.02	1.46	34.5

4.5.2. Total energy analysis of dielectric sphere

Fig 4 shows a graph of the total energy in the mill changing with time when the filling amount of the medium balls is 80% and the rotation speed is 1500rpm. The time axis starts from 0.5s because the particles are given 0.5s of sedimentation time when the initial conditions are set. It can be seen from the figure that the energy increases rapidly before t=0.6, and then gradually decreases until the energy in the mill reaches a stable value at t=1.38s, and remains unchanged at 2.87J. This shows that the grinding has entered a stable stage. Therefore, the analysis of mill-related data in the article is taken from the data after stable operation.

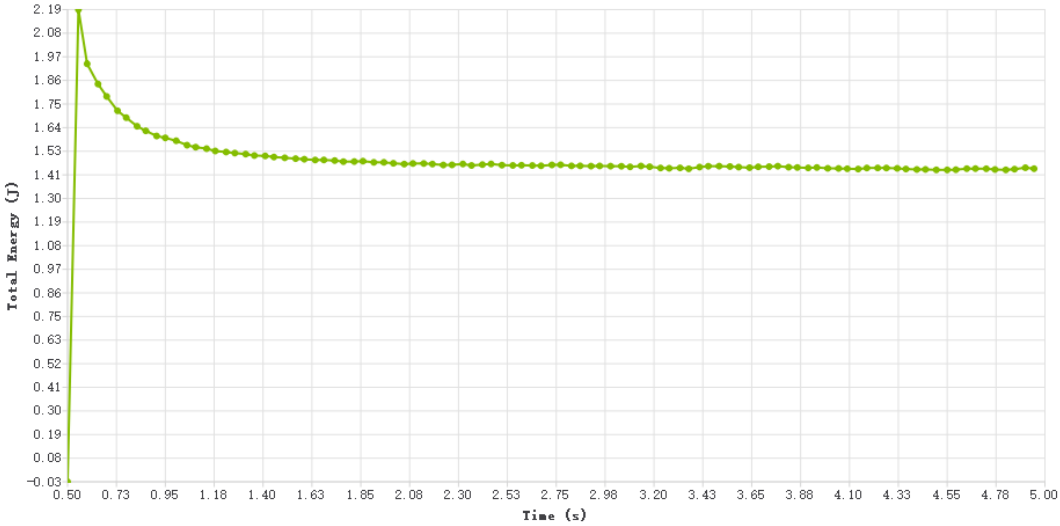

Fig 4 Changes of total energy in the mill over time

4.5.3. Force analysis of grinding media in different areas

In order to study the force of the grinding media in the radial direction, the horizontal section from the stirring shaft to the cylinder wall is evenly divided into 10 parts at intervals of 50 mm, as shown in Fig 5 (a). In Fig 5 (b), the red grinding media moves at a higher speed, while the blue grinding media moves at a lower speed or is stationary. It can be observed that the grinding media speed distribution in the AH area is uniform, which is due to the symmetry of the cross section and similar composition of this area. At the edge of the dispersion disk diameter, the grinding media has a higher speed, while the speed is lower in the central area. This phenomenon occurs because the grinding media at the edge of the dispersion disk diameter can obtain greater kinetic energy under the action of centrifugal force . The high speed of the

ISSN: 1813-4890

grinding media is conducive to the grinding of the material, which highlights the importance of the edge area of the dispersion disk diameter.

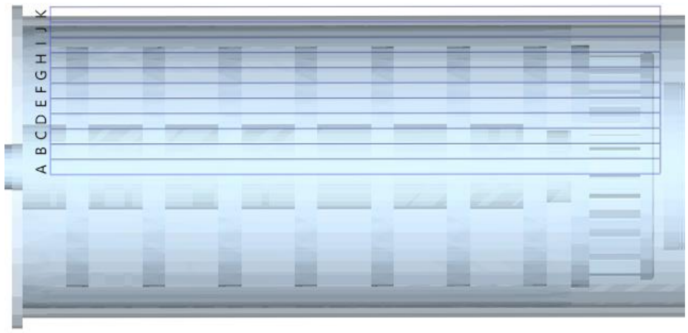

(a) Regional division

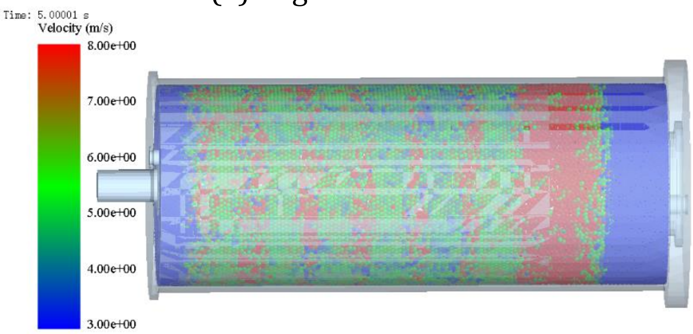

(b) Velocity gradient distribution

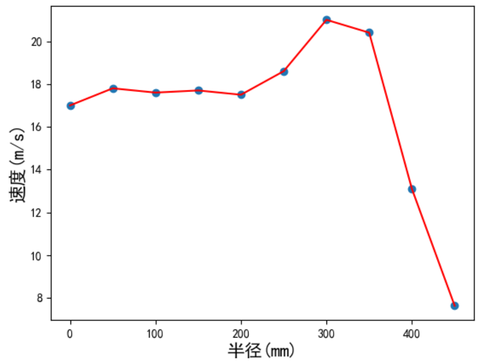

(c) Distribution of the mean velocity along the radial direction

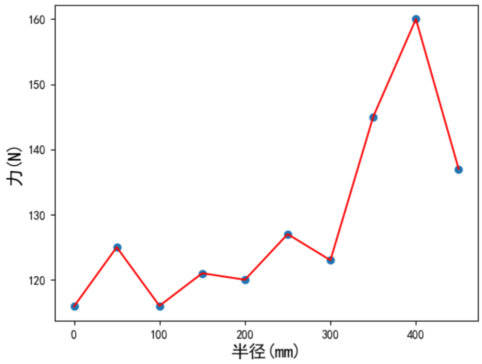

(d) Distribution of mean force along the radial direction

Fig 5 Vertical load distribution of grinding media

Fig 5 (c) shows the change in the average speed of the grinding media at different horizontal radii. In the area with a radius of less than 250 mm, the movement speed of the grinding media is maintained at about 17 m/s. However, from 250 mm to 350 mm, the grinding media speed suddenly increases. This is because there are no low-speed areas in the I and J regions, resulting in an increase in the average speed. When the radius exceeds 350 mm, the grinding media speed drops sharply because the particles in the J region have lost their power source.

Fig 5 (d) shows the average force on the grinding media at different horizontal radii. Within a radius of 300 mm, the force on the grinding media fluctuates around 125 N, which has similar characteristics to the velocity distribution. The difference is that the grinding media velocity decreases at 300 mm, but the average force only begins to increase at this time. In the radius range of 300 to 400 mm, the average force on the grinding media increases sharply and gradually decreases after the radius of 400 mm. The grinding of materials depends not only on impact crushing, but also on extrusion. Therefore, the area within a radius of 300-400 mm is also crucial to particle crushing. At the same time, the effect of gravity also needs to be considered. Under the action of gravity, the grinding media located below the dispersion disk has a greater extrusion force.

In order to explore the stress of the grinding media in the longitudinal direction, the grinding area is divided into 16 parts with an interval of 150 mm, as shown in Figure 6. According to Figure 6 (b), the first and 16th parts located at the beginning and end of the grinding area are in a low-speed motion state.

The average speed change of the grinding medium in different length directions is shown in Figure 6 (c). The speed of the grinding medium in the 2nd to 11th interval fluctuates, which is due to the uniform distribution of the dispersion disks in this area. In the 13th and 14th intervals, the speed of the particles increases significantly, which is because the structure of the last dispersion disk of the main axis is different from that of the first seven dispersion disks .

The average stress conditions of the grinding medium in different length directions are shown in Fig 6 (d). The average stress conditions of the grinding medium are similar to the changing trend of the speed.

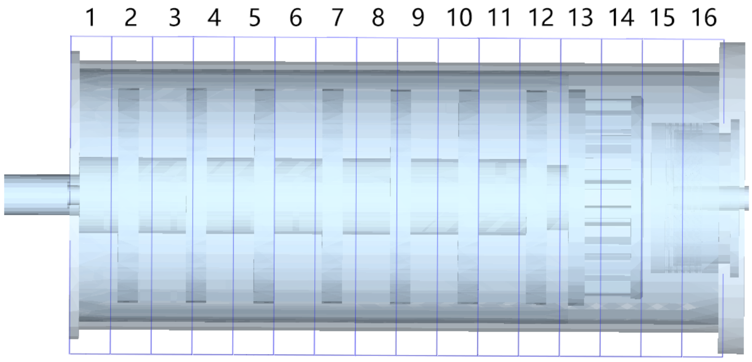

(a) Regional division

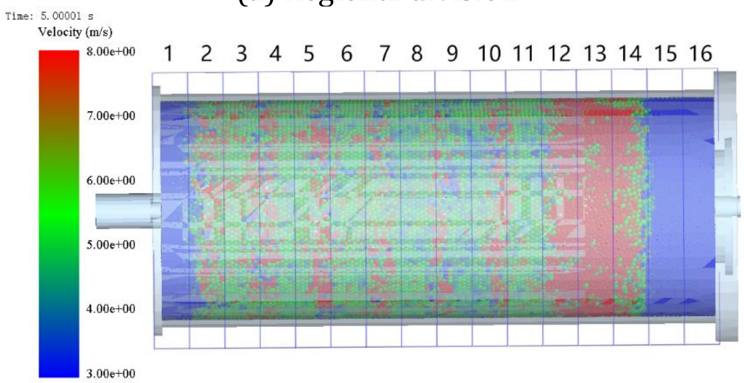

(b) Velocity gradient distribution

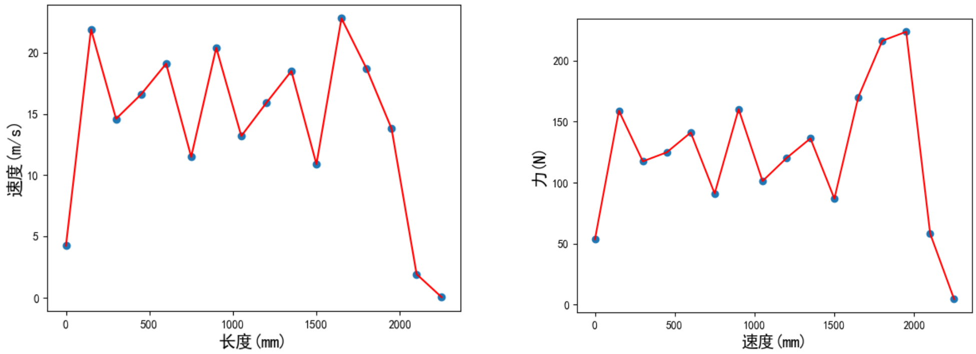

(c) Distribution of the mean velocity along the radial direction d) Distribution of mean force along the radial direction

Fig 6 Changes in horizontal load of grinding media

According to the above analysis, the speed and load of the grinding media depend on the position of the particles relative to the dispersion disk .

4.5.4. Effect of stirring shaft speed on grinding

The diameter of the grinding medium is 10 mm, the material is ignored, the filling rate is 60%, and three sets of values of spindle speed of 1000 rpm, 1500 rpm and 2000 rpm are simulated.

1. Velocity analysis of dielectric ball

According to Fig 7, as the spindle speed increases, the red grinding media gradually increases and is mainly concentrated near the dispersion disk . The increase in the movement speed of the grinding media will lead to an increase in the collision intensity, which is beneficial to the crushing of the material.

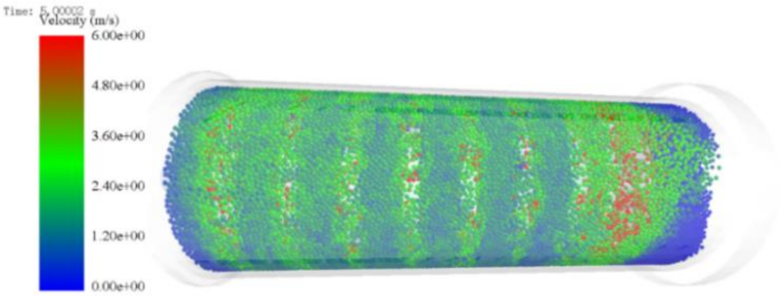

(a) Speed 1000 rpm

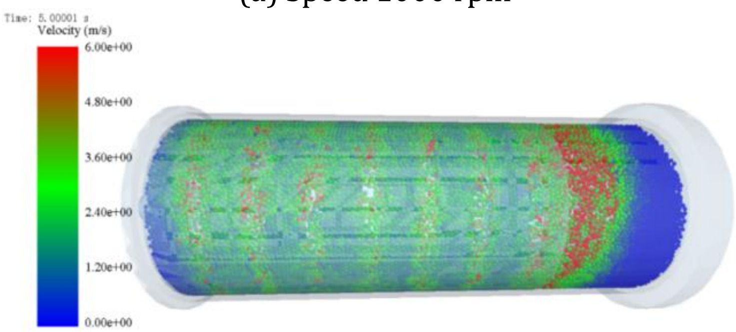

(b) Speed 1500 rpm

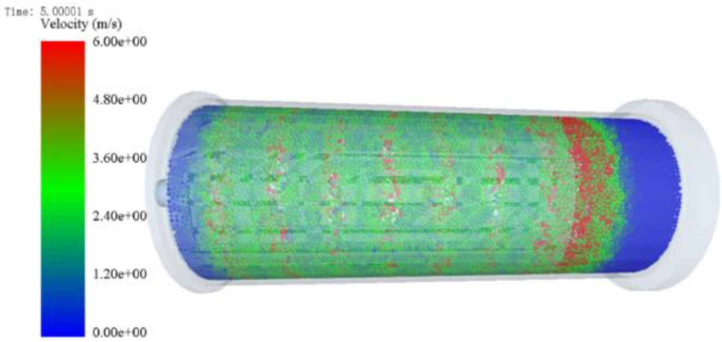

(c) Speed: 2000 rpm

Fig 7 Speed distribution of grinding media at different spindle speeds

As shown in Fig 8, the average speed of the grinding medium increases from 4.9m/s to 8.4m/s when the main shaft speed increases from 1500rpm to 2000rpm . Obviously, the increase in the speed of the stirring shaft increases the speed of the grinding medium and the collision intensity of the particles, which is conducive to the crushing of the material.

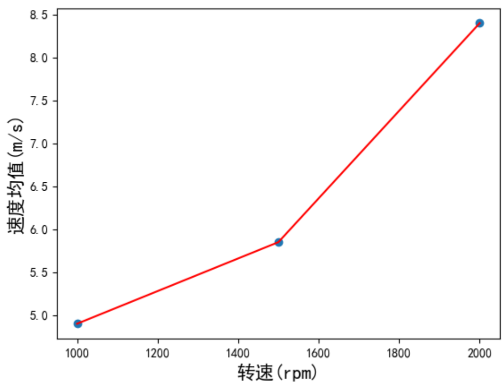

Fig 8 The influence of spindle speed on the average grinding medium speed

2. Total energy analysis of dielectric sphere

According to Fig 9, the grinding media at both ends of the cylinder are mostly blue, and the grinding media in the middle of the cylinder are mostly red and green. This shows that the medium balls near the dispersion disk have higher energy, while the two ends of the cylinder are in the low energy area. With the increase of the spindle speed, the red grinding media gradually increases and is mainly concentrated near the dispersion disk. With the increase of the movement speed of the grinding media, the blue balls in the middle of the cylinder gradually decrease, the red balls continue to increase, and the energy of the overall grinding media continues to increase.

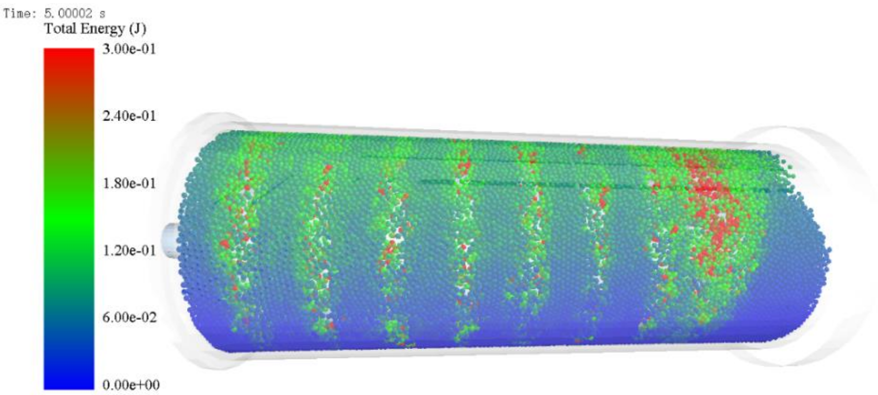

(a) Speed 1000 rpm

ISSN: 1813-4890

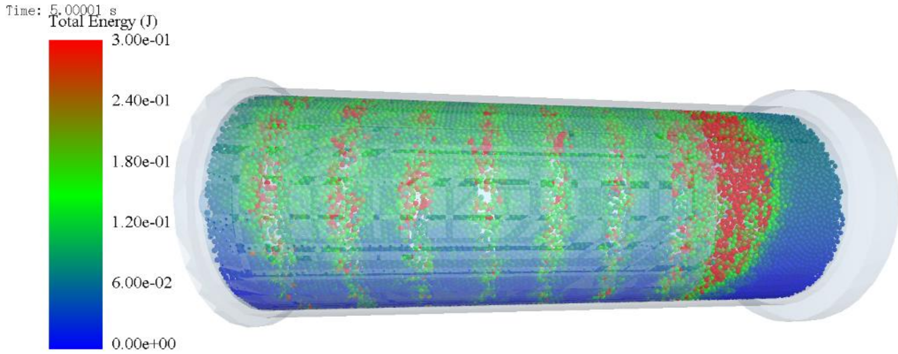

(b) Speed 1500 rpm

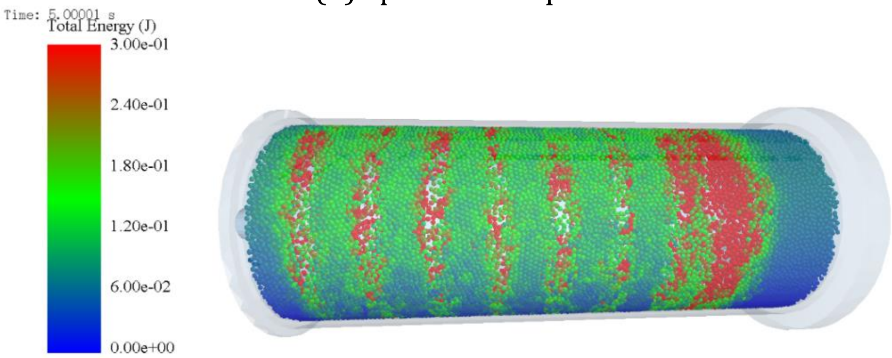

(c) Speed: 2000 rpm

Fig 9 Total energy distribution of grinding media at different spindle speeds

According to Fig 10, when the spindle speed increases from 1000rpm to 3000rpm, the average total energy of the grinding media increases from 0.73J to 2.7J. The rotation of the spindle transfers kinetic energy to the grinding media. As the spindle speed gradually increases, the kinetic energy obtained by the grinding media gradually increases, so the average total energy gradually increases. The higher the energy transferred to the material, the better the material crushing effect.

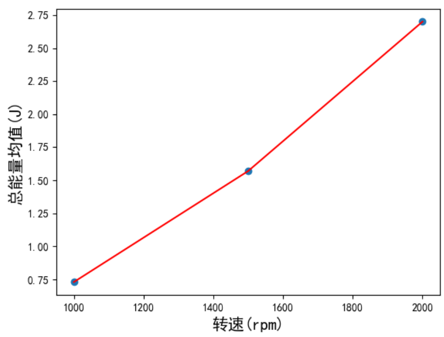

Fig 10 The influence of spindle speed on the average total energy of grinding media

3. Compression force analysis of dielectric ball

According to Fig 11, when the spindle speed is 1000rpm, the overall grinding media is displayed in green. As the spindle speed increases, the number of red spheres increases significantly, and the red spheres appear randomly without obvious rules. The compression force increases with the increase of the spindle speed.

ISSN: 1813-4890

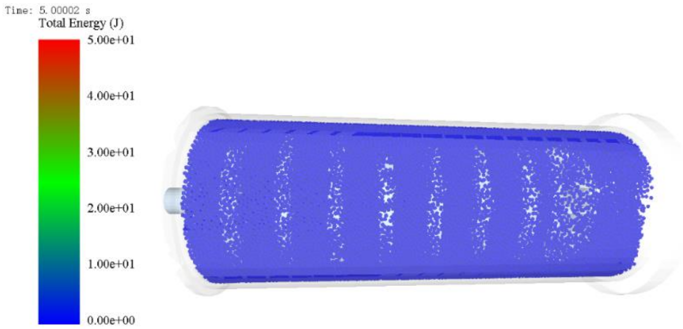

(a) Speed 1000 rpm

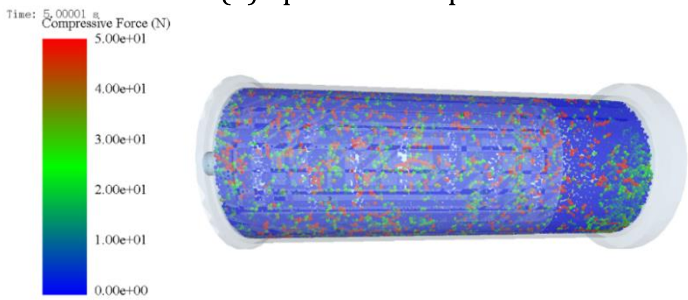

(b) Speed 1500 rpm

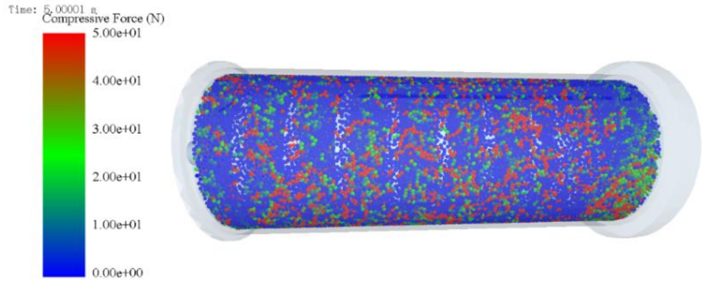

(c) Speed: 2000 rpm

Fig 11 Compression force distribution of grinding media at different spindle speeds

It can be seen from Fig 12 that when the spindle speed increases from 1000rpm to 3000rpm, the average compression force of the grinding medium increases from 26.8N to 75.5N. As the spindle speed increases, the compression force of the grinding medium also increases. The increase in compression force is conducive to the crushing of the material.

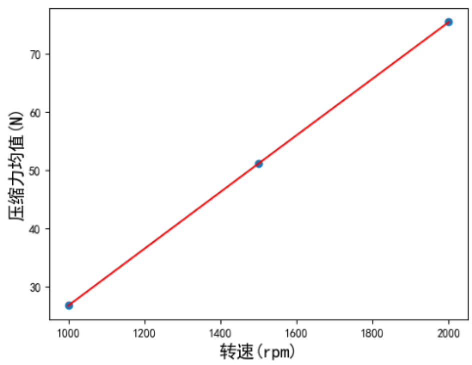

Fig 12 The influence of spindle speed on the average compression force of grinding media

5. Conclusion

This chapter designs the structure of a large-scale wet horizontal ultrafine stirred mill and establishes its simplified model. The particle field in the mill is simulated and analyzed using EDEM software, and the load of the grinding media in different areas of the mill is studied. In addition, the mill under different working conditions is simulated to study the effects of spindle speed and filling amount on particle crushing.

(1) Participated in the research and development of a large-scale wet-process horizontal ultrafine stirred mill of Henan Longbai Intelligent Equipment Manufacturing Co., Ltd. , and the stirred mill has been successfully applied in Henan Longbai Group.

(2)A discrete element analysis model of a large-scale wet horizontal ultrafine stirred mill was established to study the loading conditions of the grinding media in different grinding areas of the mill. The results show that there are two main factors that affect the speed and force of the grinding media in the mill. The first is the position of the grinding media relative to the dispersion disk . Under the action of centrifugal force, the kinetic energy and force obtained by the particles close to the edge of the dispersion disk diameter are significantly higher than those of the particles in other parts. Secondly, under the action of gravity, in the same vertical cross-section, the particles at the bottom of the mill have smaller kinetic energy, while the particles at the top of the mill have larger kinetic energy, but the particles at the bottom are subjected to greater compression force.

(3) A discrete element analysis model of a large-scale wet horizontal ultrafine stirred mill for different working conditions was established, and the effects of spindle speed and media filling amount on the grinding effect were analyzed. The research results show that increasing the filling amount of grinding media is a more effective way to improve the grinding effect than increasing the spindle speed. In the range of spindle speed from 1000rpm to 2000rpm, for every increase of 500rpm, the average speed, total energy and compression force obtained by the grinding media increased by 0.2, 0.6 and 1 times the original values, respectively. In the range of filling rate from 60% to 90%, for every increase of 10% filling amount, the average speed, total energy and compression force obtained by the grinding media increased by 0.5, 0.6 and 1.25 times the original values. In addition, increasing the material filling amount is more economical.

References

[1] Datta A, Rajamani R K. A direct approach of modeling batch grinding in ball mills using population balance principles and impact energy distribution[J]. International Journal of Mineral Processing, 2002, 64(4): 181-200.

[2] Govender I, Powell M S. An empirical power model derived from 3D particle tracking experiments[J]. Minerals engineering, 2006, 19(10): 1005-1012.

[3] Zhao D, Nezami E G, Hashash Y M A, et al. Three-dimensional discrete element simulation for granular materials[J]. Engineering Computations, 2006, 23(7): 749-770.

[4] Gui N, Fan J R. Numerical simulation of motion of rigid spherical particles in a rotating tumbler with an inner wavelike surface[J]. Powder technology, 2009, 192(2): 234-241.

[5] Gers R, Climent É, Legendre D, et al. Numerical modelling of grinding in a stirred media mill: Hydrodynamics and collision characteristics[J]. Chemical Engineering Science, 2010, 65(6): 2052-2064.

[6] Mannheim V. Empirical and scale-up modeling in stirred ball mills[J]. Chemical Engineering Research and Design, 2011, 89(4): 405-409.

[7] Conway-Baker J, Barley R W, Williams R A, et al. Measurement of the motion of grinding media in a vertically stirred mill using positron emission particle tracking (PEPT)[J]. Minerals engineering, 2002, 15(1-2): 53-59.

[8] Sinnott M, Cleary P W, Morrison R. Analysis of stirred mill performance using DEM simulation: Part 1–Media motion, energy consumption and collisional environment[J]. Minerals Engineering, 2006, 19(15): 1537-1550.

ISSN: 1813-4890

[9] Barley R W, Conway-Baker J, Pascoe R D, et al. Measurement of the motion of grinding media in a vertically stirred mill using positron emission particle tracking (PEPT) Part II[J]. Minerals engineering, 2004, 17(11-12): 1179-1187.

[10] Jayasundara C T, Yang R Y, Guo B Y, et al. CFD–DEM modelling of particle flow in IsaMills–Comparison between simulations and PEPT measurements[J]. Minerals engineering, 2011, 24(3-4): 181-187.